Modelling the variation of mechanical properties along oak boards

Cristóbal Tapia Camú, Materials Testing Institute, University of Stuttgart

Simon Aicher, Materials Testing Institute, University of Stuttgart

Keywords: timber variability, stochastic modelling, autoregressive model

1 Introduction

The study of the variation of the mechanical properties along structural lumber has been a recurring subject in the field of timber engineering for the past four decades. The results can be used straight forward in the analysis of size effects in laminations subjected e.g. to pure tension loading (*Showalter et al.*, 1987; *Lam and Varoglu*, 1991; *Taylor and Bender*, 1991; *Isaksson*, 1999), but, most importantly, the study of the length-wise variation of the material properties serves as a corner stone in the development of complex numerical strength models for glued laminated timber (GLT) beams (*Ehlbeck and Colling*, 1987; *Blaß et al.*, 2009; *Frese et al.*, 2010; *Fink*, 2014). Here, it sets the necessary underlying stochastic variability model for the laminations, which, together with the properties of the finger-joints, determines the strength characteristics of GLT beams.

Mainly two types of models are used for the simulation of the variation of properties within the boards. One comprises the use of a set of fitted linear regressions comprising a set of correlated variables, like knot area ratio (*KAR*), modulus of elasticity (MOE) and density (ρ). This is used by *Ehlbeck and Colling* (1987), *Isaksson* (1999) and *Blaß et al.* (2009) in their respective models. Alternatively, the variability can be described as an autoregressive (AR) process of different orders, where the serial correlation and cross-correlation coefficients are considered. This approach used by *Kline et al.* (1986) for the MOE variation, and *Taylor and Bender* (1991) regarding MOE and f_t variation, with AR models of order 2 and 3, respectively. Similar to the latter approach, *Lam and Varoglu* (1991) used a moving average (MA) model of order 3 for the tensile strength. The model used by Lam and Varoglu differs from an AR model by the fact that in a MA process the previous innovation values, typically representing white noise, are weighted instead of the previous computed values.

The latter type of models were calibrated by *Kline et al.* (1986), *Taylor and Bender* (1991) and *Lam and Varoglu* (1991) with data obtained from tensile tests, where window lengths between 610 mm and 762 mm were used for the measurement of MOE and/or strengths. These measurement lengths are fairly large when compared to the windows of 150 mm used to obtain the *KAR* and densities values used in the former models by *Ehlbeck and Colling* (1987). This is especially true, when the length of the boards used in some currently produced oak GLT beams can be in the same length range of around 600 mm (see e.g. ETA-13/0642 (2013)). Another problem with the models of *Kline et al.* (1986), *Lam and Varoglu* (1991) and *Taylor and Bender* (1991) consists in the explicit disregard of stiffness and strength indicators such as the *KAR* and density. These indicators, especially the *KAR* value, can be useful in a further refinement of the model.

This paper presents the first state of a newly developed stochastic model for the simulation of the variation of MOE and tensile strength along oak lumber boards. In a first part, experiments made on a total of 47 oak boards of 2.5 m length will be presented, where the MOE variation was measured over a length of 1.5 m in windows of 100 mm, giving a total of 15 measurements per board. Further, the maximum possible number of tensile strength values for each board was obtained, by successively testing the pieces not damaged after the initial failure. In the second part, an autoregressive model for the MOE and tensile strength is developed.

2 Experimental campaign with oak boards

2.1 Material

The variation of the modulus of elasticity was measured in a batch of oak boards (Quercus robur), originating from France, delivered by the company Scierie Mutelet, Rahon, France. The batch consisted of a total of 47 boards and contained a mixture of appearance grades QF2 and QF3, according to EN 975-1 (2009), which were classified in a follow-up grading at the MPA, University of Stuttgart, according to the LS strength grading classes described in DIN 4074-5 (2008). The different appearance grades enable a variable degree of *knotiness* and grain deviation in the sample, which leads to different amounts of variation in the MOE measurements of each board. The nominal dimensions of the specimens were 2500 mm × 175 mm × 24 mm (length × width × thickness) and the moisture content (measured with a pin-type resistance meter) was 10.2 % (COV = 4.6 %).

2.2 MOE and tensile strength measurements

An experimental campaign was set-up to measure the variation of the modulus of elasticity along the board and fiber direction for oak boards. A total of 47 boards were tested in tension in a servo-hydraulic universal testing machine (max. load 600 kN). The

boards were placed in the testing machine as shown in Fig. 1. The free length between the grips was about 1700 mm, providing approx. 350 mm of clamping length at both ends.

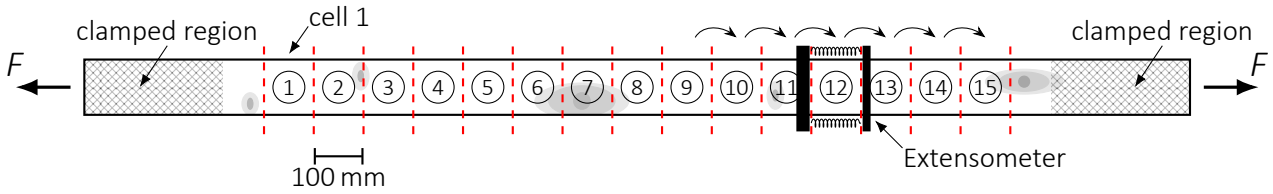

Figure 1. Used test set-up for the determination of the variation of the elastic modulus along the boards.

The free length of each board was divided into 15 *cells* (windows) of length 100 mm, and the (mean) elongation was measured for every cell by means of a specific extensometer, as shown in Fig. 1. The extensometer consists of two U-shaped steel frames, attached to the board by means of special screws, with two linear variable displacement transducers (LVDTs) placed at diagonally opposite sides of the board cross-section for the measurement of the axial deformations (see Figs. 2a,b). The respective tests started with a displacement-controlled loading of the board at a stroke rate of 0.04 mm/min and were stopped once a tensile load of 30 kN was reached. Then, the specimens were unloaded at a rate of 5 kN/s until zero load. After this, the extensometer was shifted to the next cell and the described sequence of loading and displacement measurement was repeated. The process described was performed for each cell within the free length.

In a subsequent step, the global MOE was measured over a length of 1500 mm, equal to the summed-up length of all the investigated cells in the board. This serves the purpose of checking the overall quality of the measurements at the individual cells. (Note: if the local measurements are correct, then the difference between the measured global MOE

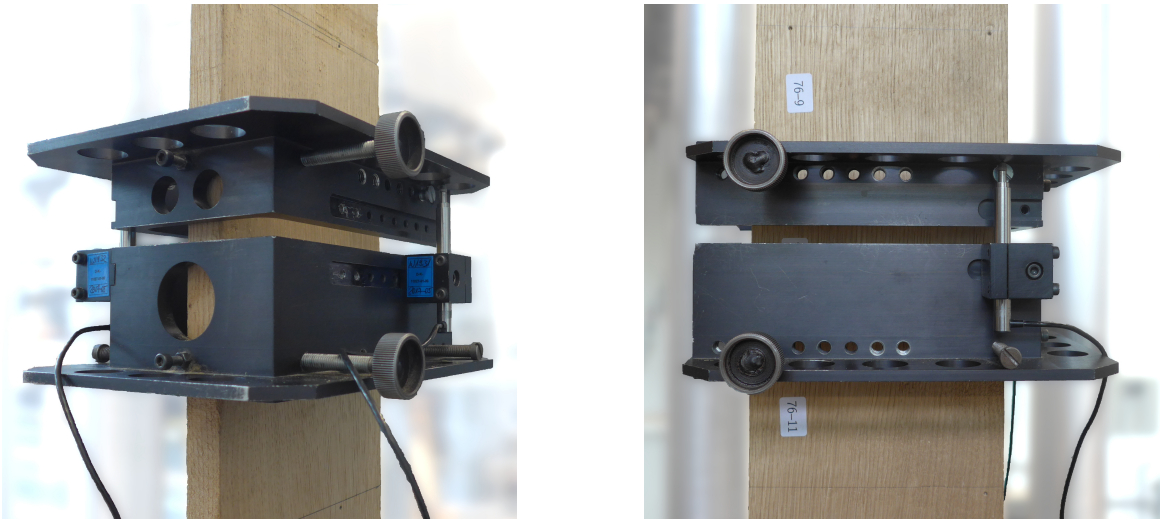

(a) *(b)*

Figure 2. Extensometer used for the measurement of the deformations in the 100 mm long cells. (a) rear-side view; (b) lateral view. The used LVDTs can be seen in both figures.

and the global MOE computed with the local measurements (cell data) should be small in relative terms.)

Finally, the boards were tested in tension until failure occurred. The position (number of the cell) where the board failed was recorded, in order to obtain a correlation between tensile strength and MOE. If the remaining pieces of the board were not damaged, another tensile test was performed on each one of the remaining parts, which allowed to gather additional information regarding the distribution of the tensile strength along the board. Due to the nature of some of the observed failures, a rigorous assignment of the *weak cell* was not always possible. Nevertheless, a careful observation during and after the test leads, in general, to the onset of the crack initiation, which most of the times can be associated with a knot or extreme fiber deviation.

2.3 Measurement of knot-related variables and grain deviation

The position and dimensions of each knot larger than 5 mm was recorded using a digital caliper gauge. For each knot, three dimensions were measured: the minimum and the maximum diameter of the assumed ellipse, and the width taken perpendicular to the principal axis of the board. These three variables allow for the later determination of the rotation angle of the knot, which is represented by an ellipse. Knots (areas) at different faces of the board, corresponding to the same knot volume, are marked with a unique number. This information is used to digitally reconstruct the geometry of the knots in each board and compute the *KAR* values for each cell, and globally, for the grading according to DIN 4074-5 (2008).

The maximum grain deviation was manually measured for each board by means of a special scriber. The determination of the grain deviation throughout the board is out of the scope of this paper, but would certainly give additional, relevant information for the MOE-tensile strength model.

3 Analysis of the experimental results

3.1 Modulus of elasticity

The longitudinal deformation measurements of each cell were used to compute the MOE values, for which the mean value of both LVDTs was taken. In the evaluation, only the data-points starting from 10 kN were considered, which helps to avoid possible non-linearities produced by slip-movements of the boards in the clamping areas at the beginning of the loading regime. The analysis of the data showed, that all measurements were within the linear range, which was proven by computed squared correlation coefficients, R^2, almost equal to unity.

Similarly, the global MOE values ($E_{glob,test}$), measured with a gauge length spanning all cells, were measured for each board and were then compared to the global MOE values

($E_{\text{glob,cells}}$) computed directly from the local MOEs. The MOE $E_{\text{glob,cells}}$ is obtained from the known equation for springs connected in series, given by

$$\frac{L_{\text{glob}}}{E_{\text{glob,cells}} \cdot A} = \sum_i \frac{\ell_{i,\text{cell}}}{E_{i,\text{cell}} \cdot A} \quad , \tag{1}$$

where L_{glob} is the reference length (1500 mm) over all 15 cells, $E_{i,\text{cell}}$ are the MOEs measured for each cell and $\ell_{i,\text{cell}}$ is the cell length (100 mm). The value A corresponds to the cross-section area and it is only shown for completeness, since it cancels out in Eq. (1). The comparison of the measured MOE with the computed global MOE showed a good agreement $E_{\text{glob,test}}/E_{\text{glob,cells}} = 1.01 \pm 0.01$.

3.2 Knot-related variables

The gathered data for the position and dimensions of the knots on the surface of the boards is processed and plotted, in order to determine pairs of knots corresponding to the same volume entity. This process was performed manually. With the data relating the pairs of knots, a 3D model of each board with its knots was produced using the python library python-occ (*Paviot*, 2018). Fig. 3 shows an example of one of these 3D models, where the knots and the respective clear wood area of each studied cell can be observed. The latter is used to compute the *clear wood area ratio* (CWAR), which is the complement of the KAR value.

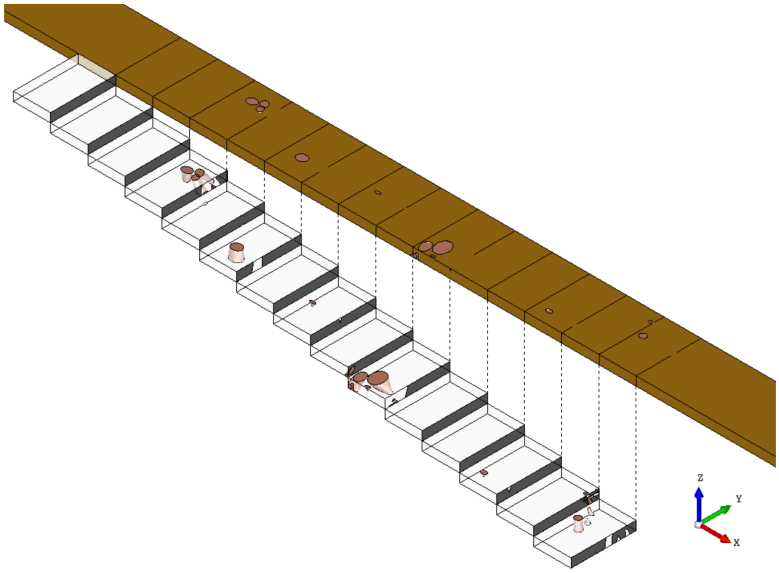

Figure 3. Post-processing of the gathered knot data, exemplary shown for board No. 50. The black areas in front of each one of the cells correspond to the respective clear wood area ratio.

3.3 Relationship between modulus of elasticity, tensile strength and CWAR

The post-processed data obtained for MOE, tensile strength and CWAR allows for an analysis of the relationships between them. Three specific relations were analyzed: (a) the one between the MOE variation and the CWAR; (b) the correlation between

tensile strength and MOE; (c) and the correlation between tensile strength and CWAR. Figs. 4a–d show the MOE and CWAR-value variation for four different tested specimens, as well as the position of the weakest sections (cells observed to be responsible of the global failure for each board). The chosen examples depict typical situations with different observed coefficients of variation (COV) for the MOEs and different CWAR variations throughout the boards.

From the information depicted in Figs. 4a–d (and from all the other boards studied) it can be clearly seen that, as expected, most of the time the boards failed in regions containing knots, which also exhibit relatively lower MOE values. It can also be seen, that large variations of MOE can be observed in absence of knots, too (see Fig. 4c), and that also in these situations the board will probably fail in this position. This indicates

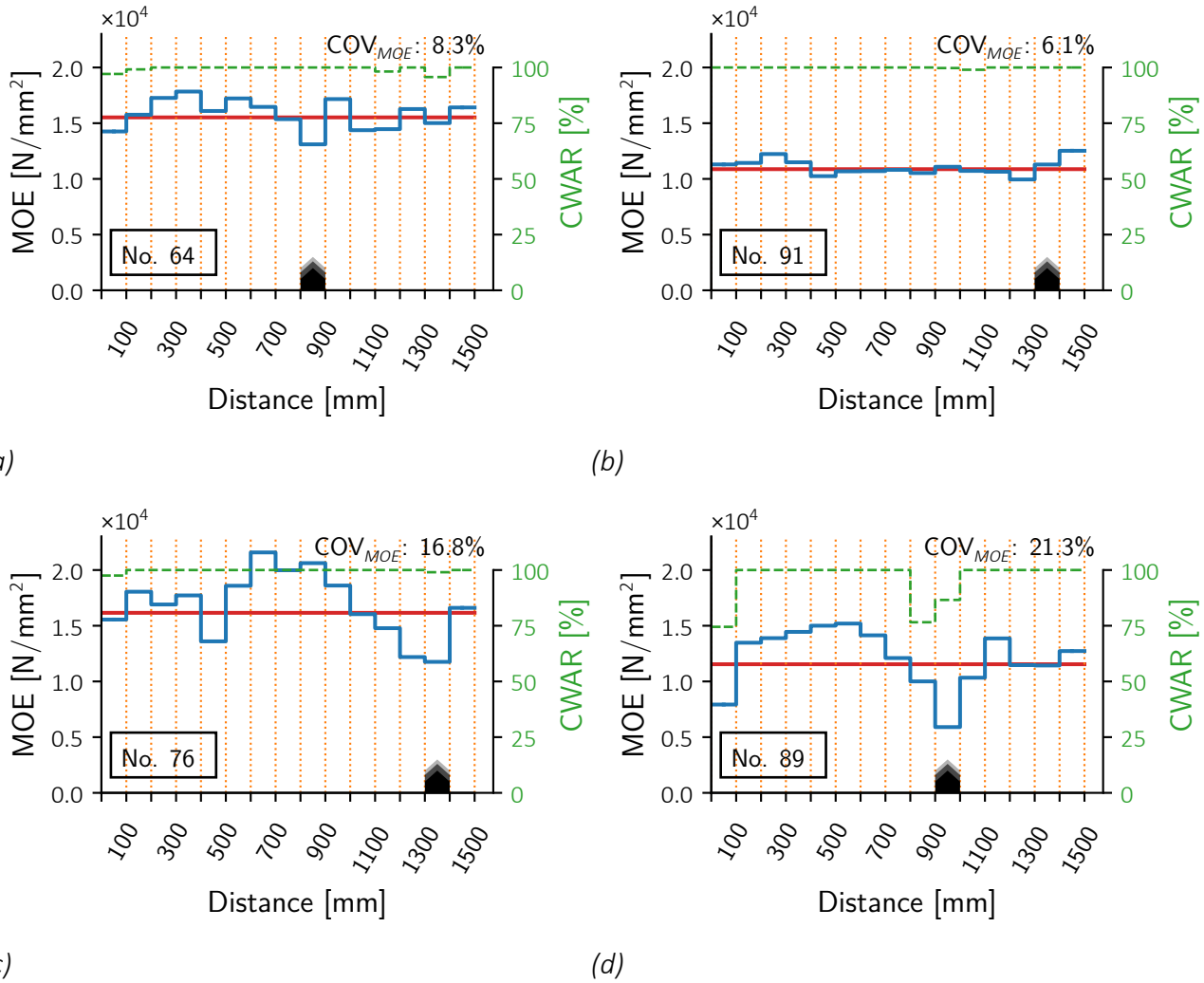

Figure 4. Variation of the measured MOE and CWAR (dashed line), weak sections and tensile strengths for different specimens. The weakest sections are marked by a black wedge at the bottom of each axis for every specimen; the red, straight line denotes the measured global MOE of all the 15 cells together ($E_{glob,test}$). (a) Specimen 64 is characterized by a relatively large COV for the MOE and a rather small correlation with CWAR values; (b) Specimen 91 shows a small COV for the MOE with no presence of knots; (c) Specimen 76 presents a high COV for the MOE which is not explained by a high knotiness; (d) Specimen 89 shows a high COV for the MOE with a very good correlation with CWAR values.

a probable correlation between the MOE and strength values at the weakest section of the board.

The correlation between global MOE of a board and its tensile strength has been shown to be low, and this was also the case in this study ($R^2 = 0.213$, see Fig. 5a). It is therefore of much interest to notice that a positive correlation between the MOE of the weakest section and the tensile strength occurring frequently in the same region is observed, reflected by a squared correlation coefficient of $R^2 = 0.509$ (see Fig.5b).

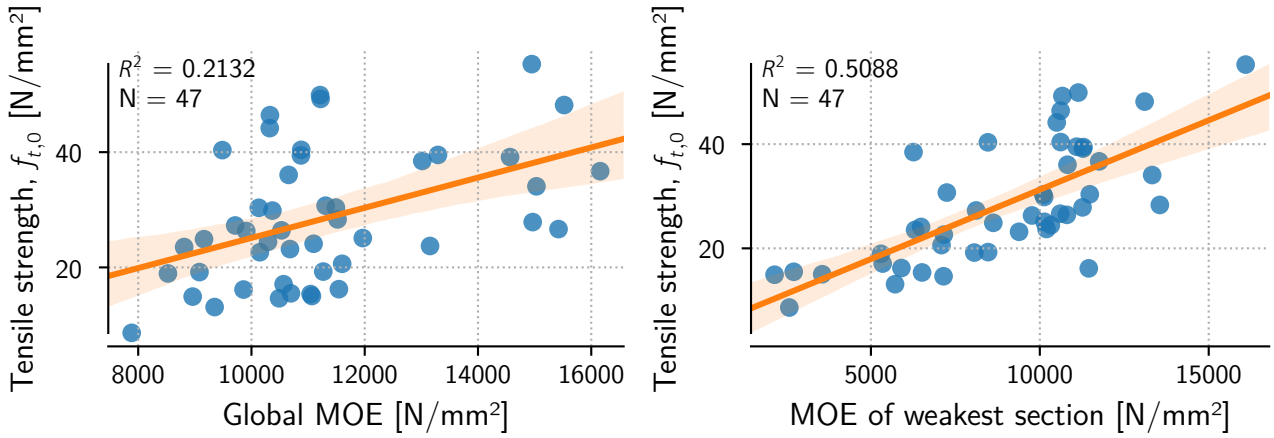

(a) *(b)*

Figure 5. Correlations between MOE and tensile strength. (a) Correlation between the global MOE vs. $f_{t,0}$; (b) local MOE measured at the weakest cell and its corresponding tensile strength.

3.4 Variation of the modulus of elasticity

As it was shown in the previous section, the MOE can present a relatively high fluctuation with respect to its *global* value. A large portion of the fluctuation can be directly attributed to the presence of knots (see e.g. Fig. 4d). However, a high variation of the measured MOE throughout the board was observed in *knot-free* regions, too (see e.g. Fig 4c). For the purpose of this paper, this variation in the *knot-free* region is considered as a *base* variation of the MOE. A deeper analysis of the *knot-free* segments would reveal the statistical characteristics of this base fluctuation, giving relevant information for the development of a model for the simulation of the MOE variation.

For the following analysis, the concept of the serial *lag-k* correlation is used, which captures the correlation between each element of a vector and the corresponding *k*-shifted element of the same vector. The serial *lag-k* correlation coefficients are computed for the MOE variation of each board, similar as done by *Showalter et al.* (1987), *Taylor and Bender* (1991) and *Lam and Varoglu* (1991). In order to capture the information concerning the base variation of the MOE, only long enough clear-wood segments are considered. This segments are defined as a minimum of 7 contiguous cells (i.e. 700 mm) in each board with a *KAR*-value below 2 %. This small accepted *KAR*-value allows for a few extra boards to be chosen for the computation of the serial correlations.

An important aspect of the method used for the computation of the serial correlations comprises the *normalization* of the MOE data of each board, so that they can all be analyzed together. This process uses the same concept presented by *Taylor and Bender* (1988) to map random variates belonging to one distribution to another one. In this case, the MOE values of each board are fitted to a normal distribution and then *mapped* into a $\mathcal{N}(0, 1)$ distribution. This process brings the MOE data from different boards to a common base level, which allows for a simultaneous analysis. It is also important to notice that the tuples (E_n, E_{n+k}), used for the computation of each *lag-k* correlation, always belong to a same board, i.e. the MOE values of the different boards are *not* concatenated into a single vector to perform the correlation. Putting all the data into a single vector would be a mistake, since cells of different boards would be mixed when computing the serial correlations.

Figs. 6a–c show the computation of the first three serial correlations for the previously defined clear wood segments. It can be noticed, that the serial correlation beyond *lag-1* is practically non-existent (see Fig. 6d) and that even for the first lag the serial correlation

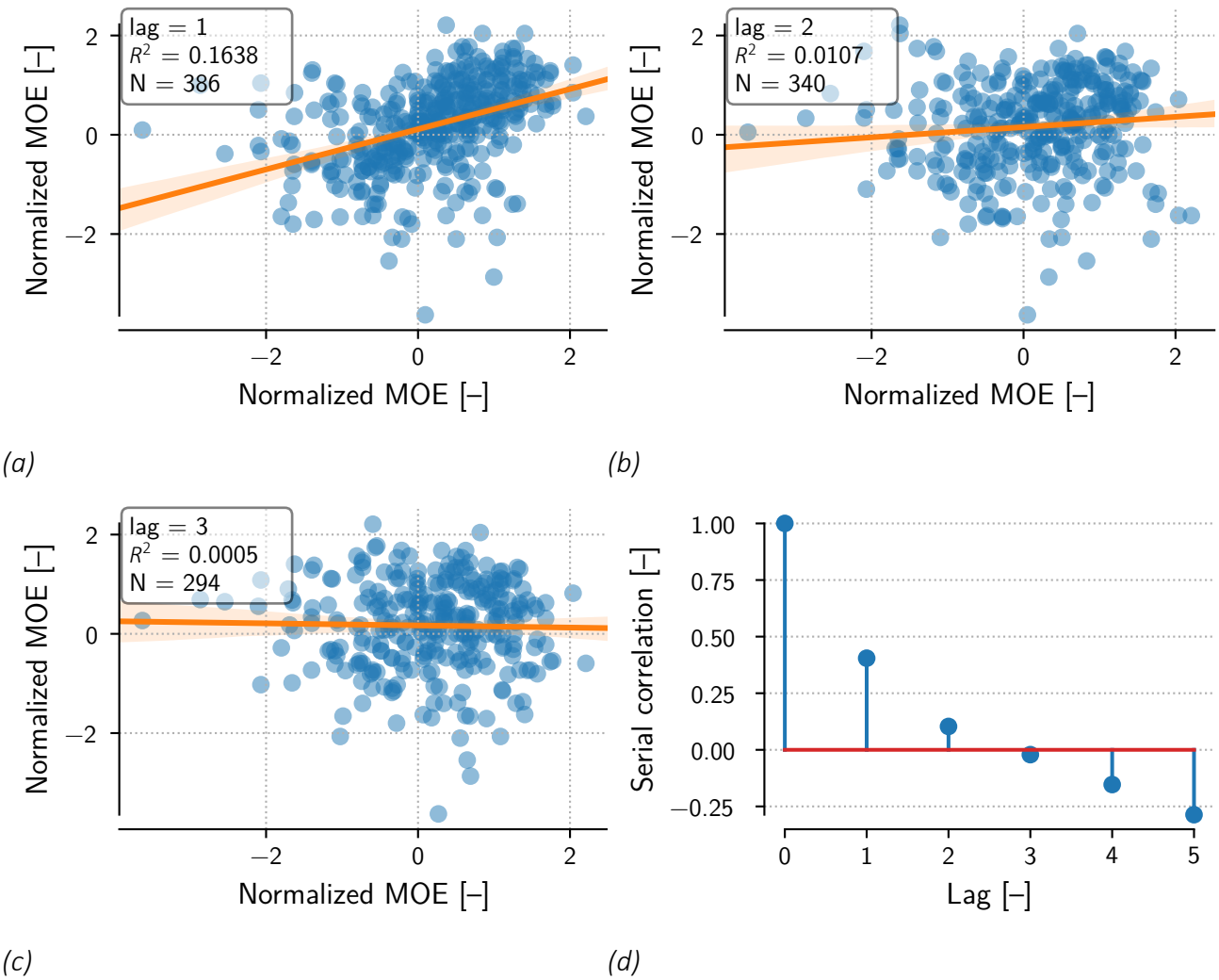

Figure 6. Linear regression used to compute the first three lags of the serial correlation (Figs. (a), (b) and (c)) and calculated serial correlations (d)

it is rather weak ($R = 0.405$). The values for the serial correlations can be taken from Table 1, where, additionally to the mentioned clear wood segments, the serial correlation coefficients for all the boards are presented (i.e. the serial correlations computed for the whole dataset, without additional filtering). From here it can be seen, that the process of filtering out the segments containing knots helps to improve the obtained serial correlation values (from $R = 0.330$ to $R = 0.405$ for the first lag).

Table 1. First five serial correlation values computed for the clear wood segments and for all the segments without making any additional filtering

	lag-1	*lag-2*	*lag-3*	*lag-4*	*lag-5*
clear wood[1]	0.405	0.103	-0.021	-0.153	-0.286
all segments[2]	0.330	0.000	-0.092	-0.170	-0.220

[1] Segments containing a minimum of 7 contiguous cells in each board with a KAR-value below 2 %.
[2] Every cell of each board is used for the analysis.

3.5 Variation of tensile strength

The estimation of the tensile strength variation along a single board presents some apparent difficulties. The most evident of which is presented by the impossibility of taking measurements in two short, consecutive regions, such as the basic units of 100 mm studied here. The second problem results from the different failure modes that can occur. In some cases cracks propagate throughout the whole board after the first failure, leaving no long enough undamaged section to be tested again.

The tests performed on the oak boards exhibited a large amount of blunt failures, which allowed to take the remaining parts and test them up to three times (only in one case four tensile strengths were obtained). The results of this process can be seen in Fig. 7a, where the boards tested in tension more than one time are presented, separated by the assigned LS-grade.

It becomes evident that the variation of the tensile strength within a single board can be extremely large. The relative increase between the strength of the weakest section and the strength(s) of other (clear wood) sections can reach the order of six (see Fig. 7b). A slight distinction is observed in this regard for the different LS grades, where grades LS10 and LS7 show larger relative differences between the strength of the weakest cell (first failure of the full board length) and the strengths obtained by testing the fractured parts. This is also somewhat expected, since a rather “good” board, denoted by a smaller size of defects, will probably have high tensile strength values throughout its length, making the variation less pronounced.

Since the weakest spots mostly coincide with the position of a knot, this information can be used to quantify the effect of knots of different sizes (or more precisely, sections with different *KAR*-values) with respect to the clear wood properties of the board. This can be

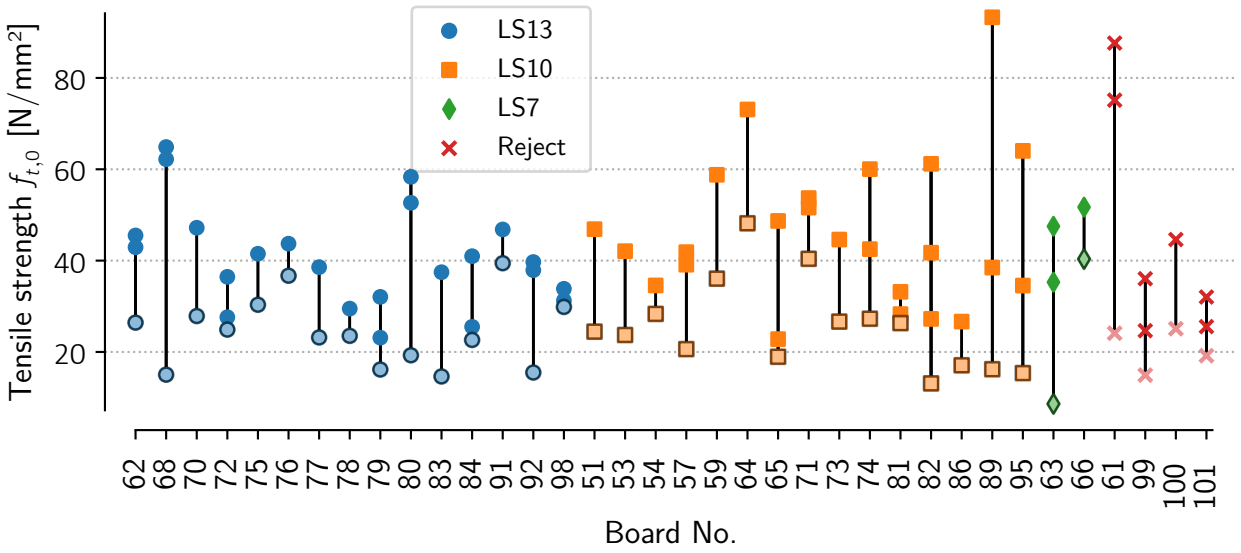

(a)

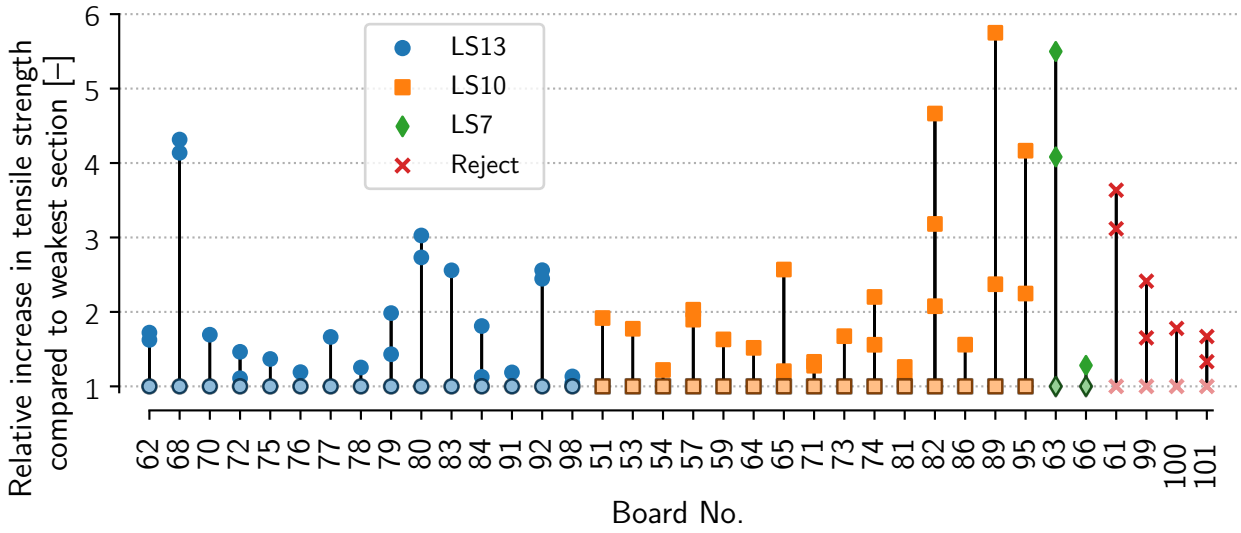

(b)

Figure 7. Variation of the tensile strength between and along individual oak boards. (a) absolute values; (b) values relative to the global failure. The results are divided into four different groups according to the classification in LS-grades (DIN 4074-5, 2008). Global failures are marked with a black edge and lighter color (always the lowest value for each board).

analyzed from different angles. Fig. 8a compares the tensile strength against the *KAR*-value. It can be seen, that no correlation is obtained. This is so, because all strengths measurements are treated equally, when they actually should be studied relative to the other strengths in the same board (each board would have a different *base* tensile strength). Another manner of observing the effect of the *knotiness* of a section is to compare this value against the relative increase observed in the maximum value of the other tested sections of the same board. Fig. 8b depicts this methodology and shows that a moderate correlation can be obtained ($R^2 = 0.454$).

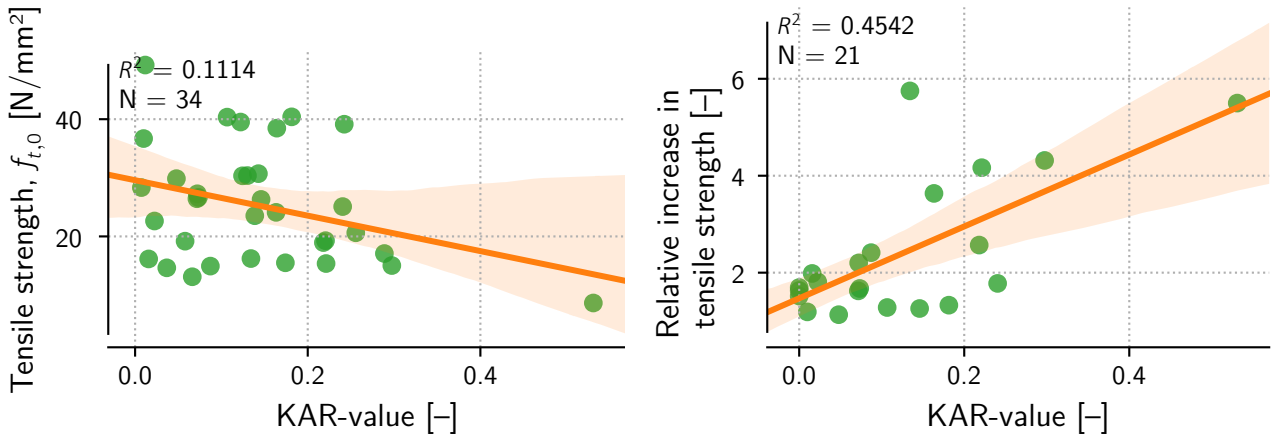

(a) *(b)*

Figure 8. (a) Correlations between KAR-values at the weakest cells and their tensile strength; (b) Correlation between KAR-values at the weakest cells and the maximum relative increase in strength for the other tested parts of the same board. Only weakest sections with KAR > 0 (N=34) were used and additional failures occurring in clear wood (N=21).

The rather moderate correlation is bound to the fact that knots do not represent the exclusive property that determines the decrease in tensile strength along the board, but interacts with other (defect) characteristics like grain deviation and density. Furthermore, as already mentioned, it is not always possible to determine the exact region where the failure began with sufficient certainty (although much care was taken to do so), which introduces an additional error to the data.

However, the shown experimental results reveal the magnitude of the variation of the tensile strength along oak boards, and their correlation with the elastic modulus and knot area ratio. This information is of high usefulness in the further development of a model to simulate the variation of both MOE and tensile strength within a board.

4 Simulation of mechanical properties along single boards

The gathered experimental data provide relevant information about the variation of the mechanical properties (MOE and $f_{t,0}$) along the studied oak boards. The next logical step consists in using this information in the development of a stochastic model to simulate this intra-board variation. In the following, it is shown how these data can be used to this end, based on the concept of an autoregressive model.

4.1 Autoregressive model applied to the simulation of MOE data

For the simulation of the MOE along the board, the approach used by *Kline et al.* (1986) and *Taylor and Bender* (1991) was implemented, which represents the variation of the MOE and tensile strength along each board as an autoregressive model. In its general form, an autoregressive model for a variable X_t (MOE or $f_{t,0}$) of order p has the form

$$X_t = C + \sum_{i=1}^{p} \varphi_i X_{t-i} + \varepsilon_t, \tag{2}$$

where the values φ_i are the parameters of the model, C is a constant and ε_t is white noise. According to the experimental results, an AR(1) model (order: 1) should be enough to reproduce the observed variability of the MOE along the board. In such case, the only parameter of the model, φ_1, takes the same value as the obtained *lag-1*-correlation, i.e. $\varphi_1 = 0.405$. This model will generate data in a normal distribution $\mathcal{N}(0, 1)$, which then can be mapped into a distribution that represents the MOE values of a given board (*Taylor and Bender*, 1988). With this, the model is fully determined and can be used to simulate any number of oak segments.

However, the data generated by the model described in general do not delivers the global value assigned to the board—i.e. the global MOE computed from the single cells will not match the MOE assigned to the whole board—, which is a result of the stochastic nature of the method. A correction is, therefore, required. For the case of the MOE, this is done by simply shifting the data so that the resulting stiffness of the board, computed from the individual values of each cell, matches the assigned global stiffness. The resulting global MOE is computed by means of Eq. (1) and the difference between this value and the assigned global MOE is calculated. This difference is then added (summed) to the generated data. In order to obtain a small error between this two values, this process has to be repeated in an iterative way. In this case, five iterations were used, then resulting in a negligible error.

4.2 Cross-correlation applied to the generation of the strength data

For the generation of the strength data along the board, the concept of a vector autoregressive model (VAR) was applied, which is used to correlate different time-series-like variables. However, differently as in a typical VAR model, the generated data are based on the already generated (autocorrelated) X_t data for the MOE. For this, the *lag-0* cross-correlation between the MOE and $f_{t,0}$ is used. The model takes the following form:

$$Y_t = C + \psi_0 X_t + \varepsilon_t, \tag{3}$$

where Y_t are the data needed to be generated (tensile strength), X_t are the data (MOE) to be correlated to and ψ_0 is the model parameter corresponding to the lag-0 cross-correlation ($\psi_0 = 0.7$). C and ε_t have the same meaning as before. Now, the reason why the MOE data are generated in the $\mathcal{N}(0, 1)$ space becomes obvious: since the $f_{t,0}$ data have to be correlated to the MOE values by means of the coefficient ψ_0, the fact that both variables correspond to the same distribution $\mathcal{N}(0, 1)$ spares the need to compute a scaling factor between two different distributions.

Similar as for the MOE-data, a correction is applied to the strength values, which consists of shifting the data so that the minimum value of each board equals the assigned strength of the board.

4.3 Application of the described simulation model

The model was applied to two different configurations of boards (*A* and *B*), which were assumed to have a different COVs for the variation in their elastic modulus and tensile strength. This COVs, together with the mean values for the MOE and minimum values for the $f_{t,0}$ are presented in Table 2. The statistical distributions used for the properties along the board correspond to *lognormal* distributions, since this ensures only positive values to be generated.

Table 2. Coefficients of variation used for the MOE and $f_{t,0}$ used for the simulations of boards A and B

	E_{mean} [N/mm^2]	$f_{t,0,min}$ [N/mm^2]	COV_{MOE} [%]	$COV_{f_{t,0}}$ [%]
Board *A*	18 000	60	5	15
Board *B*	15 000	30	15	40

Figs. 9a,b show the results of the simulations performed given the parameters from Table 2. From both figures the serial correlation in the MOE can be noticed, as well as the cross-correlation between the MOE and $f_{t,0}$. Although a setting of a high COV for the modulus of elasticity (Board *B*) could be used to simulate sudden decreases in the MOE, like the ones produced by the presence of knots (as seen in Fig. 9b), there might be a better option to do it. Namely, this could be preferably achieved by creating a low variability board (e.g. Board A, see Fig. 9a) and then include knots in a stochastic manner to reduce the properties accordingly. Nevertheless, the presented approach

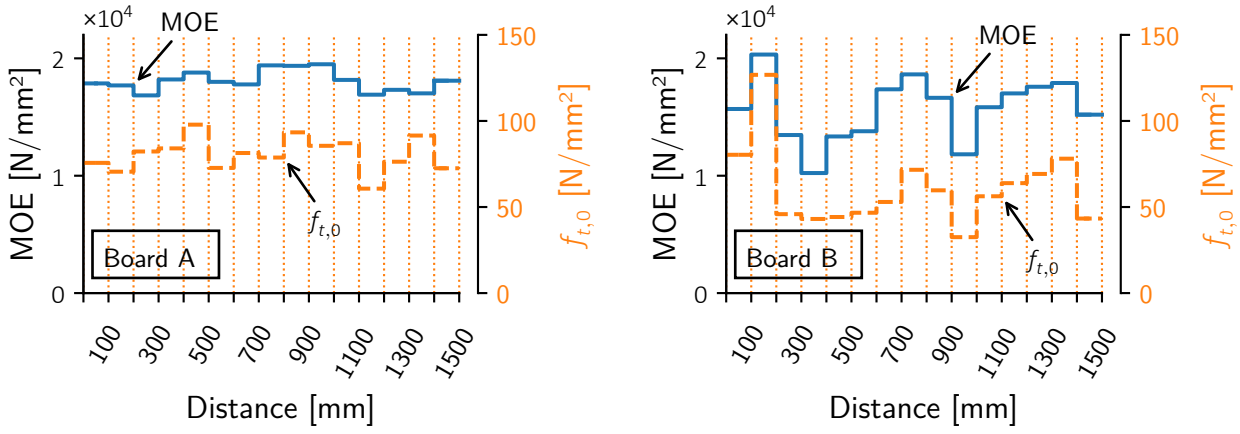

(a) *(b)*

Figure 9. Results of the simulations for the variation of MOE (continuous line) and $f_{t,0}$ (dashed line). (a) Board A: a board with low COV in the MOE (5 %) and $f_{t,0}$ (15 %); (b) Board B: a board with higher variation in its MOE (15 %) and in its $f_{t,0}$ (40 %).

shows that an autoregressive model can be used to model the stochastic variability of the mechanical properties along oak boards.

5 Conclusions

The variation of the mechanical properties (MOE and $f_{t,0}$) of oak boards was studied experimentally by means of a series of tensile tests. Measurements of the MOE over the short lengths of 100 mm allowed for the computation of serial correlation coefficients, which, for clear wood segments, yielded a *lag-1*-correlation of 0.4. Due to the low values obtained for the rest of the *lag-k* correlation coefficients, it can be assumed that a serial correlation of order larger than 1 has no relevance.

The analysis of the variation of the tensile strength within each board showed a large relative increases in the strength of the cells that failed in the secondary tensile tests. The magnitude of this increase was shown to have a relationship with the knot area ratio (*KAR*), expressed by a linear regression with a squared correlation coefficient of $R^2 = 0.45$.

Although a very low correlation between global MOE and tensile strength was observed ($R^2 = 0.21$), it could be observed that a higher correlation was obtained between the MOE of the weakest cell (the cell where the board failed) and the tensile strength ($R^2 = 0.51$).

The gathered statistical information was used for a model to simulate the variation of the MOE and tensile strength along the board. The model consists of two parts: the first part generates the MOE data by means of an autoregressive model, and the second part generates the strength values by means of a modified vector autoregressive model. Overall, the model can simulate the MOE data in a good manner, when compared to the experimental measurements, being able to replicate different COVs, depending on the type of board that is needed. A further improvement to the model would be the inclusion of a third variable accounting for the explicit location of knots along the board, which could be combined with the simulated MOE and $f_{t,0}$ values to produce more realistic results.

6 References

Blaß, H. J., M. Frese, P. Glos, J. K. Denzler, P. Linsenmann, and A. Ranta-Maunus (2009). *Zuverlässigkeit von Fichten-Brettschichtholz mit modifiziertem Aufbau, Bd. 11*. Tech. Rep. Karlsruhe, Germany: Karlsruher Berichte zum Ingenieurholzbau. DOI: 10.5445/KSP/1000008462.

DIN 4074-5 (2008). *Strength grading of wood – Part 5: Sawn hard wood*. Berlin, Germany: German Institute for Standardization.

EN 975-1 (2009). *Sawn timber – Appearance grading of hardwoods – Part 1: Oak and beech*. Brussels, Belgium: European Committee for Standardization.

Ehlbeck, J. and F. Colling (1987). *Biegefestigkeit von Brettschichtholz in Abhängigkeit von Rohdichte, Elsatizitätsmodul, Ästigkeit und Keilzinkung der Lamellen, der Lage der Keilzinkung sowie von der Trägerhöhe*. Tech. Rep. Karlsruhe, Germany: Versuchsanstalt für Stahl, Holz und Steine, Universität Fridericiana Karlsruhe.

ETA-13/0642 (2013). *European technical approval – Glued laminated timber of oak*. OIB, Vienna, Austria.

Fink, G. (2014). "Influence of varying material properties on the load-bearing capacity of glued laminated timber". PhD thesis. ETH Zürich. DOI: 10.3929/ethz-a-010294974.

Frese, M., F. Hunger, H. J. Blaß, and P. Glos (2010). "Verifikation von Festigkeitsmodellen für die Brettschichtholz-Biegefestigkeit". German. In: *European Journal of Wood and Wood Products* 68.1, pp. 99–108.

Isaksson, T. (1999). "Modelling the Variability of Bending Strength in Structural Timber – Length and Load Configuration Effects". PhD thesis. Lund Institute of Technology – Division of Structural Engineering.

Kline, D., F. Woeste, and B. Bendtsen (1986). "Stochastic model for modulus of elasticity of lumber". In: *Wood and Fiber Science* 18(2), pp. 228–238.

Lam, F. and E. Varoglu (July 1991a). "Variation of tensile strength along the length of lumber – Part 1: Experimental". In: *Wood Science and Technology* 25.5, pp. 351–359. DOI: 10.1007/BF00226174.

– (Sept. 1991b). "Variation of tensile strength along the length of lumber – Part 2: Model development and verification". In: *Wood Science and Technology* 25.6, pp. 449–458. DOI: 10.1007/BF00225237.

Paviot, T. (2018). *pythonOCC, 3D CAD/CAE/PLM development framework for the Python programming language, PythonOCC – 3D CAD Python*. (accessed May 10, 2018). URL: http://www.pythonocc.org/.

Showalter, K., F. Woeste, and B. Bendtsen (1987). *Effect of Length on Tensile Strength in Structural Lumber*. Research Report FPL-RP-482. Madison, USA: U.S. Department of Agriculture, Forest Service, Forest Products Laboratory.

Taylor, S. and D. Bender (1988). "Simulating Correlated Lumber Properties Using a Modified Multivariate Normal Approach". In: *Trans. ASAE* 31 (1), pp. 182–186. DOI: 10.13031/2013.30685.

– (1991). "Stochastic model for localized tensile strength and modulus of elasticity in lumber". In: *Wood and Fiber Science* 23(4), pp. 501–519.